Acta Cryst. (1998). D**54**, 47–57

X-ray Structure of the Zn^{II} β-Lactamase from *Bacteroides fragilis* in an Orthorhombic Crystal Form

ANDREA CARFI,[a] EMILE DUÉE,[a] RAQUEL PAUL-SOTO,[b] MORENO GALLENI,[b] JEAN-MARIE FRÈRE[b] AND OTTO DIDEBERG[a]*

[a]*LCM, Institut de Biologie Structurale Jean-Pierre Ebel (CEA-CNRS), Grenoble, France, and* [b]*Centre d'Ingénierie des Protéines, Université de Liège, Liège, Belgium. E-mail: otto@ibs.fr*

(*Received 4 March 1997; accepted 23 June 1997*)

Abstract

β-Lactamases are extracellular or periplasmic bacterial enzymes which confer resistance to β-lactam antibiotics. On the basis of their catalytic mechanisms, they can be divided into two major groups: active-site serine enzymes (classes A, C and D) and the Zn^{II} enzymes (class B). The first crystal structure of a class B enzyme, the metallo-β-lactamase from *Bacillus cereus*, has been solved at 2.5 Å resolution [Carfi, Pares, Duée, Galleni, Duez, Frère & Dideberg (1995). *EMBO J.* **14**, 4914–4921]. Recently, the crystal structure of the metallo-β-lactamase from *Bacteroides fragilis* has been determined in a tetragonal space group [Concha, Rasmussen, Bush & Herzberg (1996). *Structure*, **4**, 823–836]. The structure of the metallo-β-lactamase from *B. fragilis* in an orthorhombic crystal form at 2.0 Å resolution is reported here. The final crystallographic R is 0.196 for all the 32 501 observed reflections in the range 10–2.0 Å. The refined model includes 458 residues, 437 water molecules, four zinc and two sodium ions. These structures are discussed with reference to Zn binding and activity. A catalytic mechanism is proposed which is coherent with metallo-β-lactamases being active with either one Zn ion (as in *Aeromonas hydrophila*) or two Zn ions (as in *B. fragilis*) bound to the protein.

1. Introduction

β-Lactamases are defensive enzymes produced by bacteria. They catalyse the hydrolysis of the β-lactam ring of the antibiotics of the penicillin and cephalosporin families. The compounds hydrolyzed are no longer effective against their targets, membrane-bound transpeptidase enzymes (PBP). Therefore, β-lactamases represent the major cause of bacterial resistance against the β-lactam antibiotics.

The class B β-lactamases have initially received little attention because this class of enzymes was produced by only relatively innocuous *Bacillus cereus* strains. More recently, identification of some zinc β-lactamase producing pathogenic strains of *Bacteroides fragilis*, *Aeromonas*, *Serratia*, *Stenotrophomonas* (*Xanthomonas*) has increased the interest for this class of enzymes. The fact that class B enzymes hydrolyse almost all the β-lactam antibiotics, including carbapenems, and that they are not sensitive to the classical β-lactamase inhibitors underlines their clinical relevance. Moreover, the same plasmid-encoded enzyme has been found in *Enterobacter*, *Serratia*, *Pseudomonas* and *Klebsiella* strains and the spreading of such plasmid-encoded enzymes to other pathogenic bacteria is a frightening possibility which stresses the importance and urgency of finding effective inhibitors.

The metallo-β-lactamases are monomeric except for the *Stenotrophomonas* enzyme which is tetrameric. The *B. fragilis* enzyme seems to be the most dangerous since it has large k_{cat} and k_{cat}/K_M values against a broad spectrum of substrates. By contrast, the *Aeromonas* enzyme has an extremely narrow specificity and is only effective against imipenem and ampicillin (Felici *et al.*, 1993). The resolution of an increasing number of crystallographic structures of class B enzymes and eventually of their complexes with substrate analogs can help in understanding their catalytic mechanism and different substrate specificities. It also represents the first step in the rational design of efficient inhibitors. In this paper we present the refined structure of the *B. fragilis* β-lactamase and a comparison with the *B. cereus* enzyme structure; some important active-site residue changes, differences in zinc affinity and consequences for the catalytic mechanism are also discussed.

2. Experimental

The crystals of the *B. fragilis* enzyme used in this study were grown at pH 9.0 in the presence of zinc as described earlier (Carfi *et al.*, 1997). The crystals are orthorhombic, in space group $P2_12_12_1$ with unit-cell parameters a = 48.086, b = 98.052, c = 111.764 Å, and two molecules per asymmetric unit. A set of diffraction data to 2.8 Å (30 250 observed reflections, 11 666 unique reflections R_{merge} = 10%, 86.3% completeness) was collected on a Fast detector at room temperature. A self-rotation function (*POLARRFN* written by Kabsch, in the *CCP*4 program suite, Collaborative Computational Project, Number 4, 1994) indicated the presence of two

Table 1. *Data-processing and model-refinement statistics*

Resolution (Å)	35–2.0
No. of observed reflections	191117
No. of unique reflections	32806
No. of unique reflections (10–2.0 Å)	32501
Completeness (%)	94.9
R_{merge} (%)/⟨Redundancy⟩	6.8/6.0
R factor (10–2.0 Å no σ cutoff)	19.6
R_{free} (10–2.0 Å no σ cutoff)	26.2
Total No. of residues	458
No. of water molecules (B<70 Å^2)	437
R.m.s.d. bonds (Å)	0.014
R.m.s.d. angles (°)	1.612

molecules in the asymmetric unit related by a 178° rotation around a non-crystallographic rotation axis which is almost perpendicular to the c axis (Carfi *et al.*, 1997).

The structure was determined by the molecular replacement method with the program *AMoRe* (Navaza, 1994) using the 2.8 Å room temperature data set and a polyalanine search model based on the refined 2.2 Å resolution structure of the *B. cereus* β-lactamase. The data in the resolution range 12–3.5 Å were used. The highest two peaks (correlation coefficient of 15.4 and 13.5, next highest 7.5) of the rotation function (Patterson cut-off radius of 25 Å) were used for the translation function. One solution for the two molecules was obtained with a correlation coefficient of 28.9% and an R = 52.7%. Rigid-body refinement with *X-PLOR* (Brünger, 1992) using data between 10 and 3.5 Å followed by a positional refinement lowered the crystallographic R factor to 49.1% and the R_{free} to 48.7% (free set represents 5% of the data). Then a $(2|F_{obs}| - |F_{calc}|, \alpha_c)$ electron-density map was computed to 2.8 Å with averaged phases calculated using the option *AVERAGE* of *DM* (Collaborative Computational Project, Number 4, 1994). A mask calculated by *MAMA* in the *O* suite (Jones, Zou, Cowan & Kjeldgaard, 1991), weights from *SIGMAA* (Read, 1986) and phases calculated from the polyalanine model were used as input to *DM*. The map clearly showed the electron density for many of the side chains, parts of the main-chain loop between β-strands β_3 and β_4 (this loop is disordered in the *B. cereus* enzyme structure and was omitted in the search model) and for some additional C-terminal residues. Moreover, electron density was observed in the active site for two closely positioned metal ions which has been interpreted as two zinc ions.

2.1. *Model building and refinement*

At this point the model for one of the molecules was built using the *B. fragilis* metallo-β-lactamase sequence with the program *O* on an ESV graphics station and the second was obtained by applying the non-crystallographic symmetry (NCS). Alternating cycles of manual rebuilding, rigid body and conventional positional refinement with NCS constraints using *X-PLOR* decreased the R_{cryst} to 37% and the R_{free} to 41% for a model devoid of the β_1 β_2 (7–11) and the $\beta_3\beta_4$ (26–36) loops. Finally these loops could be built on a *SIGMAA*-weighted $(2|F_{obs}| - |F_{calc}|, \alpha_{calc})$ omit map (Read, 1986). Ten cycles of manual rebuilding and positional refinement with NCS constraints first and tight restraints in the last cycles followed by restrained individual B-factor refinement decreased the R_{cryst} to 22.2% and the R_{free} to 28.5%.

Crystals of *B. fragilis* β-lactamase were flash-frozen after rapid soaking in the solvent of crystallization supplemented with 20%(*v*/*v*) glycerol and a 2.0 Å resolution data set was collected at 100 K, on a MAR Research image-plate area detector. The data were indexed and integrated using the *XDS* program (Kabsch, 1988) (data-collection statistics are presented in Table 1). The *CCP*4 suite was used for further processing. Several cycles of rigid-body refinement, manual rebuilding followed by NCS restrained positional refinement and then restrained individual B-factor refinement, were performed. Later the two molecules were refined independently. Charged residues and zinc ions were refined as neutral and no restraints were applied between the zinc ions and its ligands. When the R_{cryst} dropped to 26.5% and R_{free} to 29.7% water molecules were localized using the *ARP* program (Lamzin & Wilson, 1993) and refined with *X-PLOR*.

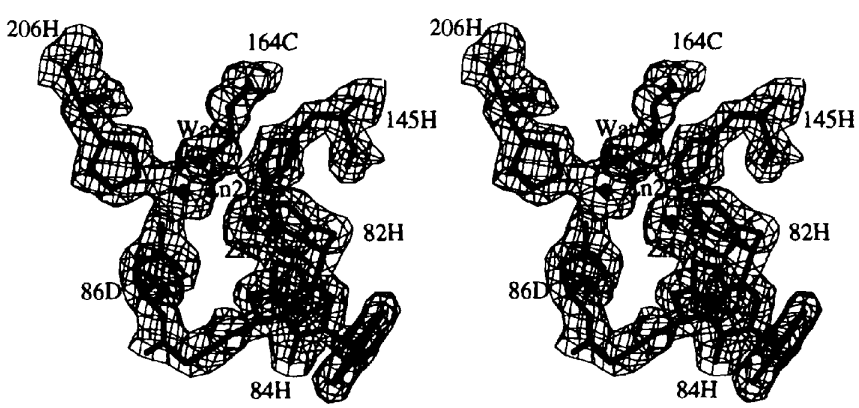

Fig. 1. Stereoview of the electron-density map of the active site. The zinc ions and their ligands are represented. The electron-density map is contoured at 1.4σ level. The figure was obtained using the *O* program.

2.2. *The tetragonal form*

After a few weeks the orthorhombic crystals spontaneously dissolved and were replaced by small cubic shaped crystals. The new crystals belonged to the tetragonal space group $P4_32_12$ with $a = b = 77.73$ and $c = 141.57$ Å with two molecules in the asymmetric unit. This crystal form is very similar to that reported by Concha *et al.* (1996) who detailed the structure of *B. fragilis* β-lactamase but did not describe the corresponding packing. Thus, it was decided to analyse the tetragonal crystals in order to verify if they were more suitable for the preparation of complexes with inhibitors. A 3.5 Å resolution data set (5732 reflections, 93.3% completeness) was collected on a MAR Research image-plate area detector. Data were processed as for the orthorhombic form. The program *AMoRe*, using one *B. fragilis* metallo-β-lactamase molecule as search model and data in the range 15–3.5 Å, gave one solution for the two molecules in the asymmetric unit with a correlation of 67.3% and an $R_{cryst} = 34.2\%$. No further refinement of the obtained solution was performed but a detailed packing comparison with the orthorhombic form could be performed.

3. Results and discussion

3.1. *Quality of the structure*

Fig. 1 shows the active site from our 2.0 Å $(2|F_{obs}| - |F_{calc}|, \alpha_{calc})$ electron-density map superimposed upon the model. The final model comprises two molecules with a total of 458 residues (out of 464), 437 molecules with *B* factors lower than 70 Å^2, four zinc and two sodium ions. The resolution (2.0 Å) of the structure described here compares well with that of Concha *et al.* (1996) whose quoted resolution (1.85 Å) seems to be overstated. Actually, for the data used in the present work a maximum value of 0.15 was allowed for R_{sym} in the highest retained resolution shell. Using the same criterion the structure of Concha *et al.* (1996) would be considered to be at about 2.1 Å resolution: their R_{sym} was 0.274 in the 2.12–1.97 Å shell and 0.398 in the 1.97–1.85 Å shell. Therefore, the differences observed between the structures in the tetragonal and orthorhombic forms cannot be ascribed to the resolution of the data.

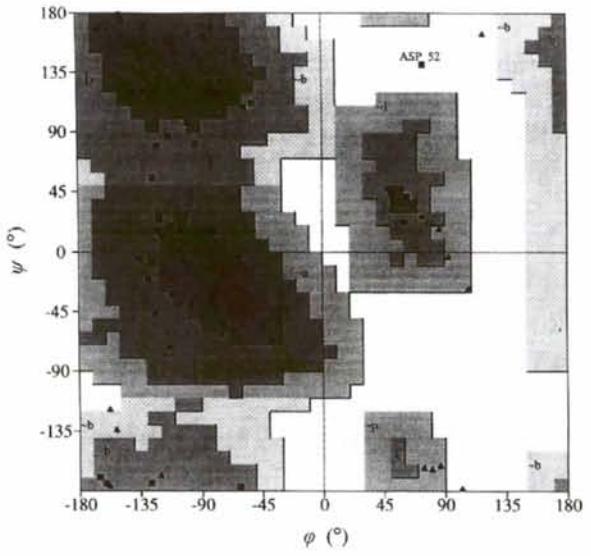

Fig. 2. Ramachandran plot calculated using *PROCHECK* (Laskowski, 1993) for the molecule *A* of the asymmetric unit. Glycine residues are shown as triangles and the other residues as squares. The Asp52 residue with conformational angles outside allowed regions is labelled.

3.2. *Accuracy of the model*

The R_{cryst} for the current model is 19.6% (using all data, 32 501 unique reflections, 10–2.0 Å) and R_{free} is 26.2%. The r.m.s. deviation from ideal stereochemistry is 0.014 Å for bond lengths and 1.612° for bond angles. The estimated r.m.s. coordinate error according to *SIGMAA* is 0.216 Å (Read, 1986). The model was checked using the program *PROCHECK* (Laskowski, 1993). For all criteria used by *PROCHECK* the model was either better or within the limits of the typical values for 2.0 Å or higher resolution refined structures. The final model has been deposited with the Protein Data Bank (Bernstein *et al.*, 1977).†

The main-chain torsion angles (φ,ψ) are represented on a Ramachandran plot (Ramachandran, Ramakrishnan & Sasisekharan, 1963) in Fig. 2. Only one residue (the

† Atomic coordinates and structure factors have been deposited with the Protein Data Bank, Brookhaven National Laboratory (Reference: 1BMI, R1BMISF). Free copies may be obtained through The Managing Editor, International Union of Crystallography, 5 Abbey Square, Chester CH1 2HU, England (Reference: LI0260).

Fig. 3. Ribbon diagram of the *B. fragilis* metallo-β-lactamase. Figs. 3, 4, 6, 8, 9, 10 and 11 were obtained using *MOLSCRIPT* (Kraulis, 1991).

Asp52 in both molecules) was in a disallowed region with $\varphi = 72$ and $\psi = 141°$. This residue is at a 90° turn of the chain, near the end of a β-strand at the opening to the active site and may have a role in the enzymatic activity. The equivalent Asp56 in the *B. cereus* and in the tetragonal *B. fragilis* structures have very similar torsion angles. The importance and details of its interactions will be discussed below. However, for one molecule, Asp125 was reported in Concha *et al.* (1996) to have dihedral angle values corresponding to a disallowed region (78,−78°). The same amino acid was found, for the two molecules, in an allowed region (−115,−70°) in the present structure. The conformation observed by Concha *et al.* (1996) is results from a different orientation of the main-chain carbonyl group of Thr124.

3.3. *Description of the structure*

The molecules (*A* and *B*) show the same four-layered α/β/β/α structure (Fig. 3) as observed for the *B. cereus* enzyme (Carfi *et al.*, 1995) and *B. fragilis* in the tetragonal crystal form (Concha *et al.*, 1996). This fold is reminiscent of the N-terminal nucleophile family (Brannigan *et al.*, 1995), the Ser/Thr phosphatases PP1 (Egloff, Cohen, Reinemer & Barford, 1995; Goldberg *et al.*, 1995), PP2B (Griffith *et al.*, 1995; Kissinger *et al.*, 1995) and PP2C (Das, Helps, Cohen & Barford, 1996), DNase I (Suck, Oefner & Kabsch, 1984; Oefner & Suck, 1986), and exonuclease III (Mol, Kuo, Thayer, Cunningham & Tainer, 1995). However, these proteins differ in their secondary-structure topologies, indicating different evolutionary origins.

The β-sandwich consists of two β-sheets (strands β_1 to β_8 and strands β_9 to β_{13} respectively) related by an intramolecular twofold symmetry (Carfi *et al.*, 1995) and is flanked on one side by parallel helices α_1 and α_2, and by helix α_3, and on the other side by antiparallel helices α_4 and α_5. Helices α_1, α_2, α_3 and the first β-sheet define the N-terminal domain, the second β-sheet and helices α_4 and α_5 the C-terminal domain. A superposition of the two molecules (Fig. 4) shows that the loop Ser25–Val35 has a different conformation (it is involved in different packing contacts for the two molecules), and that the C-terminal helix is oriented slightly differently, probably due to its binding in the active site of the neighbouring molecule (see below). Discarding these zones, the r.m.s. deviation for the Cα atoms is 0.32 Å. The numbering scheme for the secondary-structure elements is adopted from Concha *et al.* (1996), who describe an additional β-strand (β_8: residues His121 to Phe123) in the first β-sheet: the corresponding region in the *B. cereus* β-lactamase is not a β-strand due to a number of amino-acid differences which affect the side-chain packing in the interior of the protein (Ile108 in *B. fragilis* → Ala in *B. cereus*, Phe123→Leu, Leu127→Thr) or the hydrogen-bond pattern (Gly122→Asp, Tyr102→His, Ser101→Ala) (Carfi *et al.*, in preparation). It is worth noting that Val202 (belonging to strand β_{13}) makes hydrogen bonds with Gly210: Val202 N···Gly210 O (2.75 Å) and Val202 O···Gly210 N (2.89 Å) typical of antiparallel strands, which may suggest the possible presence of a 14th strand in some metallo-β-lactamases although it is not well formed in the *B. cereus* and *B. fragilis* enzymes. Fig. 5 shows the hydrogen-bonding and secondary-structure assignments for the *B. fragilis* enzyme produced by the program *HERA* (Hutchinson & Thornton, 1990).

Mostly, hydrophobic residues fill the volume between β-sheets and between the helices and the β-sheet of each domain. However, some polar residues are also buried in these interfaces: Tyr23, Ser25, Ser37, Asp52, Thr60, Asn81, Cys87, Cys138, Asp148, Asn149 and Thr218. Some of these residues are associated with internal water molecules.

3.4. *Cavities in the structure*

Concha *et al.* (1996) mentioned three clusters of non-protein atoms within the protein interior containing: one

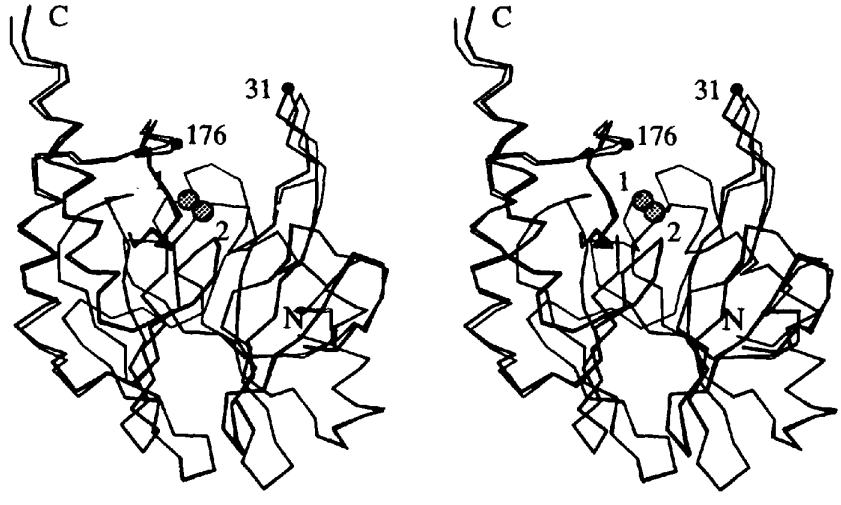

Fig. 4. Stereoview of the superposition of the two independent molecules. Labels 1 and 2 refers to Zn1 and Zn2 (see text). The distance between the Cα atoms of residues 31 and 176 varies from 14.2 to 12.9 Å between the open and closed form.

sodium ion and three water molecules; two water molecules; and one water molecule, respectively. In the present structure ten internal water molecules and one ion (tentatively identified as a Na^+ ion from the buffer) were found in seven cavities within the protein. One isolated cavity contains one water molecule hydrogen bonded to Pro135 O, Thr156 N and Thr156 OG1, involved in stabilizing interactions between strand β_{10} and the loop following strand β_{11}. An equivalent internal water molecule is found in the same position in the *B. cereus* enzyme (Carfi *et al.*, in preparation). Most of the buried polar residues, the internal sodium ion and the other nine water molecules positioned in the other six cavities contribute to the correct architecture of the Zn ions environment and of the active site by correctly orienting most of the Zn ligands (His82, His84 and His145 for Zn1, Asp86, Cys164 and His206 for Zn2) or of the residues possibly involved in the catalytic activity (*e.g.* Asn176).

Fig. 6 and Table 2 describe the interactions of the protein atoms with the sodium ion and the internal water molecules. Two of the three clusters mentioned by Concha *et al.* (1996) seem to correspond to the first two cavities of Table 2. Data in Table 2 point to the important role of Asp52 which acts as a bridge between cavities 1 (occupied by the sodium ion and three water molecules)

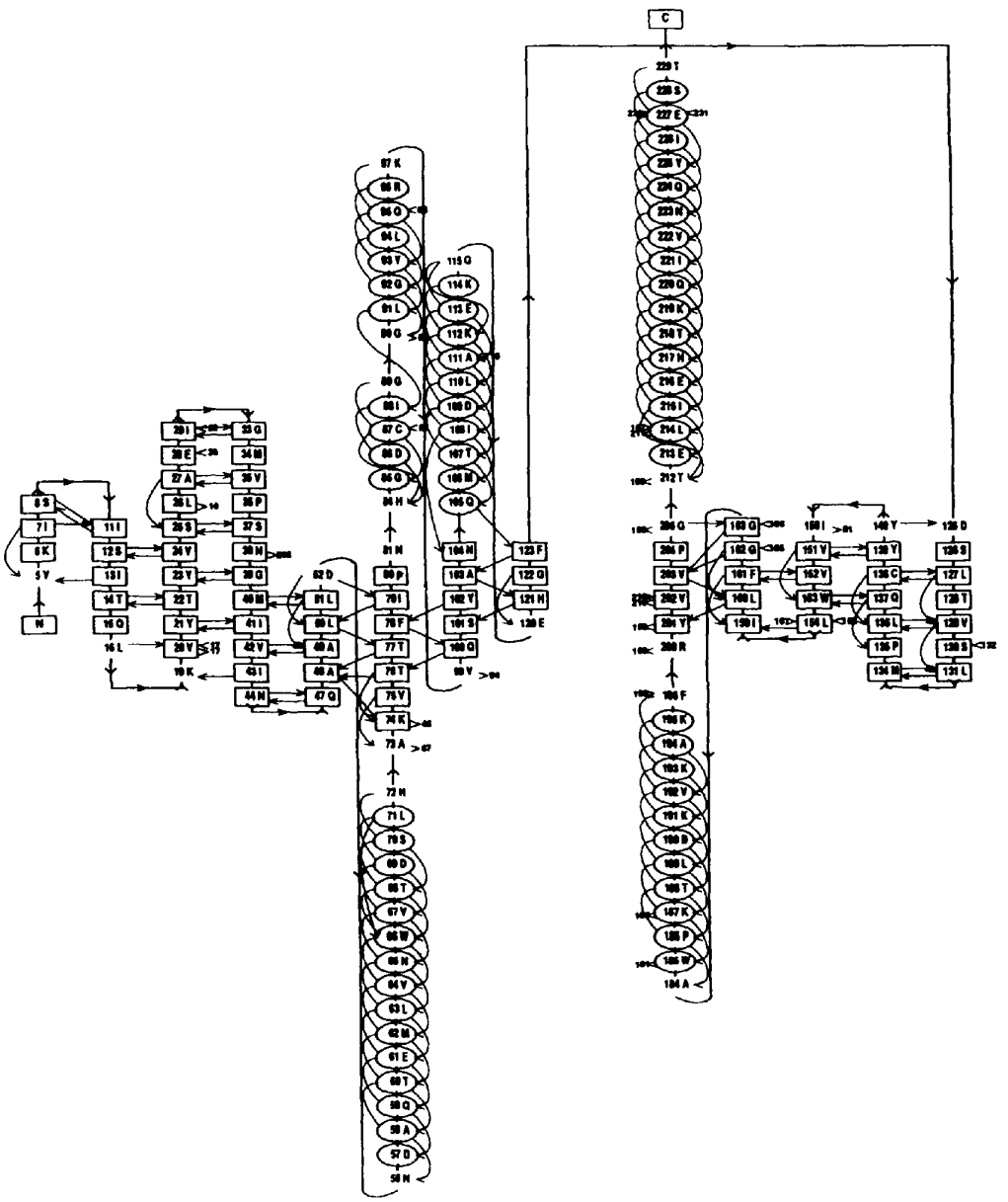

Fig. 5. Secondary structure and hydrogen bonding within the *B. fragilis* β-lactamase structure. The diagram was prepared using the program *HERA* (Hutchinson & Thornton, 1990).

Table 2. *Contents of the internal cavities in B. fragilis β-lactamase*

Cavity	Cavity content	Ligands†
1	Na^+	Asn38 O, Asp52 OD2, Asp86 O, Wat1, Wat2
	Wat1	Na^+, Asp86 OD2, Gly205 O
	Wat2	Na^+, Tyr23 OH, Ser37 OG, Thr53 O
	Wat3	Asp52 OD2, Cys164 N
2	Wat4	Asn81 ND2, Wat5
	Wat5	Asp52 OD1, Ile79 O, Wat4
3	Wat6	His145 O, Asn176 O, Asp179 N
4	Wat7	Leu141 N, Gly142 O, Asn149 O
5	Wat8	Asn81 OD1, Gly162 O, Met165 N
6	Wat9	Pro80 O, Asn104 N, Thr107 OG1

† The maximum ligand–water distance is 3.4 Å.

and 2 (occupied by two water molecules). Through the water molecules to which it is hydrogen bonded, Asp52 stabilizes Cys164 (a Zn2 ligand), and Asn81 (whose side chain interacts with His82, a Zn1 ligand). Asp52 also forms a direct hydrogen bond with Asn81 N by its OD1 atom. In the *B. cereus* enzyme, Asp52 (Asp56 in the *B. cereus* numbering, Fig. 7) is also present, but there is no metal ion similar to the sodium ion observed here since the replacement of the Cys87 residue of the *B. fragilis* enzyme by an Arg residue provides the necessary protein-stabilizing positive charge. In the *A. hydrophila* enzyme, Asp52 is replaced by a Gly residue (Fig. 7), and the stabilization of the Arg residue may be due to the Tyr residue replacing Phe161, with possible additional internal water molecules.

3.5. *The environment of the Zn ions*

The Zn ions have the same environment in the two molecules of the asymmetric unit. Each molecule contains two Zn ions, Zn1 and Zn2, located at distances of 3.35 and 3.38 Å in molecules *A* and *B*, respectively. Zn1, which corresponds to the high-affinity Zn ion in the *B. cereus* enzyme (Carfi *et al.*, 1995) is coordinated by His82 NE2, His84 ND1 and His145 NE2. Zn2 is coordinated by Asp86 OD2, Cys164 SG, His206 NE2 and one water molecule. Table 3 lists the distances between the Zn ions and their ligands. In addition to the numerous interactions with the internal water molecules (see above and Table 2), the residues involved in Zn binding and in the active-site architecture are also stabilized by a network of hydrogen bonds between protein atoms, sometimes also involving surface water molecules. As an example the side chain of Asn149 makes hydrogen bonds to His145 N (a Zn1 ligand) and Gly142 O.

For the four histidine residues liganding the Zn ions, the imidazole N atoms which are not bound to the Zn ion are all involved in hydrogen bonds to O atoms of the protein or to O atoms of a water molecule: His82 ND2···Asn81 OD1, His84 NE1···Asp179 OD2, His145 ND2···Wat10, His206 ND2···Pro36 O. Wat10 in turn interacts with the carbonyl O atom of Asn176 and Leu174 and, together with Wat6 (Table 2), helps positioning the 172–184 loop. The same residues and the same pattern of hydrogen bonds is found in the *B.cereus* enzyme with the exception of Asn81 which is replaced by Thr85 (a water molecule replaces Asn81 OD1 and in turn makes a hydrogen bond with Thr85 OG1 and His82 ND2).

The loop β6–α2 (which comprises Zn ligands His82, His84 and Asp86) and helix α2 (Leu91–Lys97) are stabilized by hydrogen bonds Trp83 N···Asp148 OD2 (3.1 Å), His84 NE2···Asp179 OD2 (2.7 Å), Trp93 N ···Asp57 OD1 (3.2 Å) and Arg96 NH2···Asp57 OD2 (3.0 Å). The same arrangement of hydrogen bonds on both ends of the zone 81–97 is found in *B. fragilis* and *B. cereus* β-lactamases, and may favour a correct orientation of the Zn binding and active-site residues. In a similar way, in glyceraldehyde-3-phosphate dehydrogenases, multiple hydrogen bonds arrangements on both ends of helices α3 and α8 contribute to the correct architecture of the NAD binding site (Duée *et al.*, 1996). This observation may explain why mutants D57V, D148V and D179V of *B. fragilis* β-lactamase show an impaired zinc binding ability although none of the mutated residues is involved in Zn binding (Crowder, Wang, Franklin, Zovinka & Benkovic, 1996).

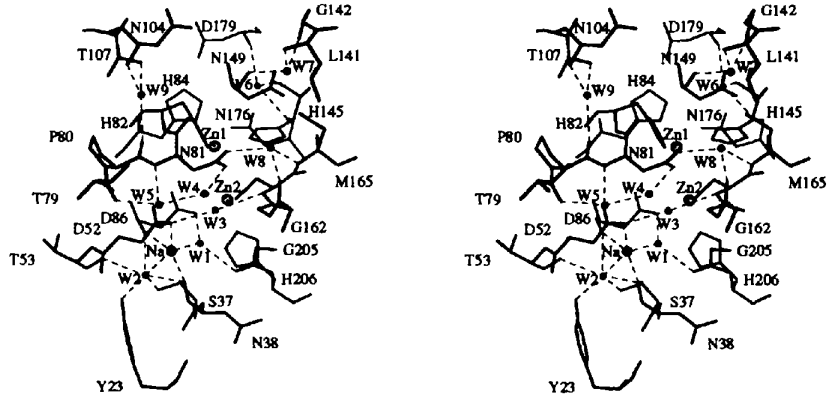

Fig. 6. Stereoview showing the internal water molecules and the Na ion and their interaction with the protein atoms.

Although the Zn2 ligands appear to be involved in fewer interactions with protein atoms than are the Zn1 ligands, the binding strength seems to be similar for both Zn ions since the temperature factors for the Zn ions and their ligands are similar. This is consistent with the fact that K_d values are both lower than 10 μM (Crowder *et al.*, 1996).

The water molecule found in the ligand sphere of Zn2 corresponds to the water molecule identified as Wat3/Wat4 in Concha *et al.* (1996). The authors described an additional site considered as occupied by a 'shared hydroxide' Wat1/Wat3, in close contact with both Zn ions, at 1.9 Å from Zn1 and 2.1 Å from Zn2. In the present structure, a difference Fourier map actually shows some positive difference density in a position corresponding to this hydroxide, but also opposite to this position with respect to each of the Zn ions, which is suggestive of an anisotropic vibration of the Zn ions. Moreover, if O atoms are added in the position of the expected hydroxides they refine with temperature factors > 42 Å^2, while the Zn ions and their neighbouring atoms refine with temperature factors <12 Å^2. The absence of the 'shared hydroxides' in the present structure of the *B. fragilis* enzyme, as compared to the structure described by Concha *et al.* (1996), could come from different crystallization conditions: the pH is 9.0 in this work and 7.0 in Concha *et al.* (1996).

Another water molecule is found in the active site and hydrogen bonded to Asn176; its distances to Zn1, Zn2 and Asn176 ND2 are, respectively, 3.42, 3.87 and 2.82 Å

Table 3. *Metal–ligand distances (Å) for the two molecules in the asymmetric unit*

Ligand	Metal	Molecule *A*	Molecule *B*
His82 NE2	Zn1	2.31	2.21
His84 ND1	Zn1	2.26	2.19
His145 NE2	Zn1	2.24	2.23
Wat_{Zn1}	Zn1	3.42	3.54
Asp86 OD1	Zn2	2.14	2.22
Cys164 SG	Zn2	2.39	2.40
His206 NE2	Zn2	2.26	2.23
Wat_{Zn2}	Zn2	2.37	2.36

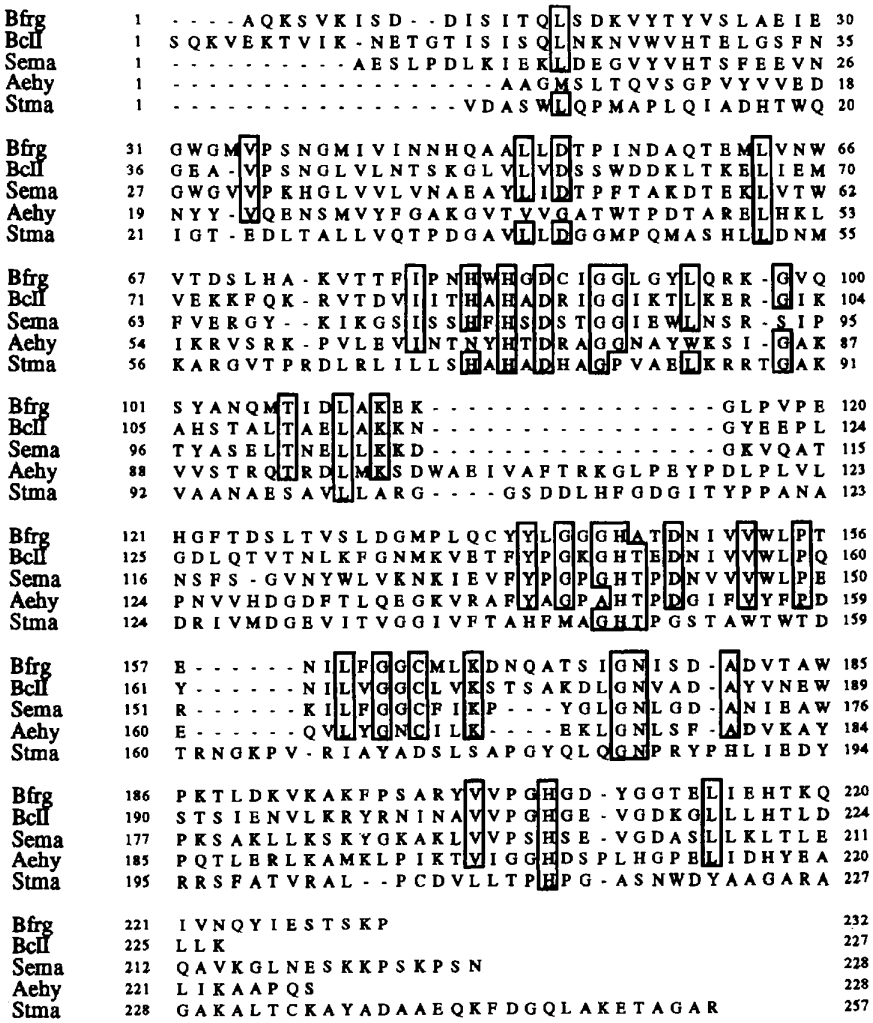

Fig. 7. Sequence alignment for some class B enzymes. For the *B. cereus* and *B. fragilis* metallo-β-lactamases the alignment is based on the superposed crystallographic structures. For the other sequences the alignment was made as described in Carfi *et al.* (1995). Sequences are: Bfrg (*B. fragilis*), BCII (*B. cereus*, 569H9), Sema (*Serratia marcescens*), Aehy (*Aeromonas hydrophila*) and Stma (*Stenotrophomonas maltophilia*).

in molecule *A*, and 3.57, 4.21 and 2.87 Å in molecule *B*. The published data do not allow to decide if the structure described by Concha *et al.* (1996) also contains this water molecule. Finally, it is interesting to observe that the equivalent water molecule in the *B. cereus* structure is displaced and is now bound to Zn1 (2.25 Å) while Asn180 presents a different rotamer and is no longer hydrogen bonded to this water molecule.

3.6. *Crystal packing of the orthorhombic crystal form*

The asymmetric unit contains two molecules labelled *A* and *B*. The packing can be described as columns of molecules stacked parallel to the *a* axis, with molecules *A* located at ($y = b/4$ or $3b/4$; $z = 0$ or $c/2$) and molecules *B* located at ($y = 0$ or $b/2$; $z = 0$ or $c/2$). The two molecules of the asymmetric unit are related by a rotation of 178.6° around an axis nearly perpendicular to the *c* axis, at 35° from the *b* axis ($\omega = 91.8°$, $\varphi = -145.1°$ as defined by the *LSQKAB* program from *CCP*4). A molecule *B* has no contact with crystallographically equivalent *B* molecules. On the contrary molecules *A* share one hydrogen bond: Arg96 O···Gln220 NE2 (2.96 Å). Most of the packing interactions occur between molecules *A* and molecules *B*. There are four regions where these contacts are non-equivalent. Viewed from molecule *B*, these are: residues Glu28 and Gly33 against Glu113 from molecule *A*; residues Asn45-His46 against Lys187 and Asp190 from *A*; residues Asn56-Asp57-Ala58 against Asp18 from *A*; residues Lys193-Ala194 and Pro197 against Asp9, Glu28 and Met34 from *A*; in particular residues Glu28 of molecules *A* and *B* make different interactions with their neighbouring molecules. The most interesting and most extensive contacts are found in the two regions where molecules *A* and *B* pack along non-crystallographic symmetry axes. In the first region (Fig. 8) the non-crystallographic axis relates the β-sheets of the two molecules in such a way that strand β_9 of the second β-sheet of one molecule packs along strand β_8 of the first β-sheet of the other molecule, resulting in the two β-sheets extending over the two molecules. The molecular contact is about 20 Å long. The non-crystallographic symmetry is well obeyed, extending to the side-chain atoms. Besides the main-chain interactions, there is a hydrophobic patch in the centre of the contact region (involving the side chains of Tyr102 and Leu127, which are on the edge of the hydrophobic interface between the two sheets of a molecule) flanked on both sides by hydrophilic patches involving on one side Gln100 and Tyr102 and one water molecule on the non-crystallographic axis, and on the other side Thr124-Asp125-Ser126 and two water molecules located on the axis. In the second region (Fig. 9) the C-terminal helix of one molecule fits into the active site of the other molecule, giving the two independent views of the active site which have been discussed above. Numerous water molecules are present in this contact zone. The non-crystallographic symmetry is much less strict than in the first region: the C-terminal helices are about 5° away from each other after fitting the two molecules, and some side chains have different conformations. Moreover, in molecule *A* no density (at the 1σ level) is present for the Lys231 side

Fig. 8. Stereoview showing the most extended contact region between molecules related by one twofold non-crystallographic axis. The twofold non-crystallographic axis is perpendicular to the plane of the figure.

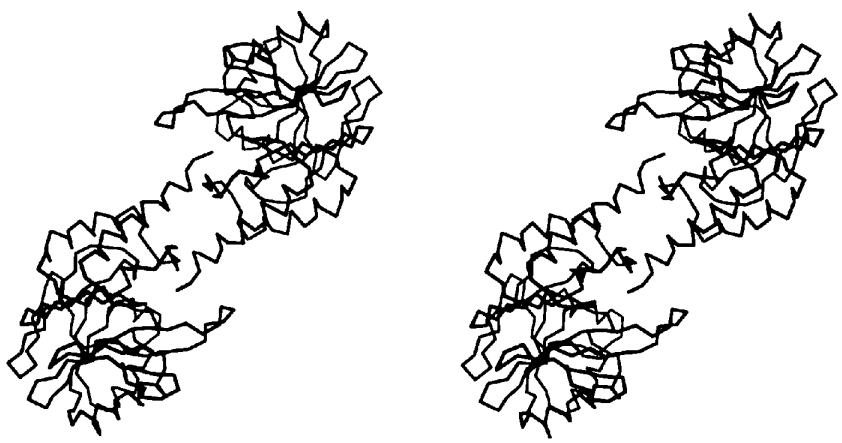

Fig. 9. Stereoview showing the C-terminal helix of one molecule fitting into the active site of the other molecule. The twofold non-crystallographic axis is perpendicular to the plane of the figure.

chain and for Pro232; by contrast these two C-terminal residues are well defined in molecule *B*. The superposition of the two molecules in the asymmetric unit (Fig. 4) shows that the active site of molecule *B* is slightly more open than in molecule *A*. Although the difference between the two molecules is obviously due to crystal packing, it is worth noting that thermolysin shows a similar closure of the cleft upon binding of substrate (Holland *et al.*, 1992). The observation of two conformations with differently opened clefts in metallo-β-lactamase may suggest a similar closure of the cleft during enzymatic activity. In agreement with this observation are the lower *B* values and better map of the C-terminal helix of molecule *B* in the active-site cleft of molecule *A* (which corresponds to the closed form).

3.7. *Comparison between the packing in the $P4_32_12$ and in the $P2_12_12_1$ forms*

In both crystal forms an almost identical asymmetric unit can be defined (molecules 1 and 2 of Fig. 10), except for a slight relative rotation of these two molecules. The most interesting point is that the interactions between molecules 1 and 2 are similar, involving the insertion of the C-terminal helix into the active-site cleft of the neighbouring molecule. The presence of the same local molecular arrangement in both crystal forms may indicate that the molecules of metallo-β-lactamase have a tendency to form that kind of interaction, at least under the crystallization conditions. To define more precisely the crystallographic correspondence between the two crystal forms (Fig. 10), the asymmetric unit (molecules 1 and 2) and the neighbouring molecules (1′ and 2′) were superposed, which corresponds to superposing the non-crystallographic twofold axis of both crystal forms. The resulting r.m.s.d. on Cα atoms is 1.85 Å while the r.m.s.d. is only 1.0 Å if only molecules 1 and 2 are considered (this results from the slightly different relative orientations of molecules 1 and 2). The superposition reveals that one diagonal of the (*a*, *b*) face (vertical in Fig. 10) of the tetragonal crystal (length 108.9 Å) is parallel to the *c* axis of the orthorhombic crystal (length 111.4 Å), while the other is parallel to one diagonal of the (*a*, *b*) face of the orthorhombic crystal (length 106.0 Å). However, apart from the non-crystallographic twofold axis, no crystallographic symmetry elements can be superposed. On the contrary, the relationship between molecule 1 and 1′ (and respectively 2 and 2′), are quite different in the two crystals: in the orthorhombic crystal form, molecules 1 and 1′ are related by the 2_1 symmetry axis parallel to *c*; in the tetragonal form, 1′ is generated from a molecule 1 (after cell translation) by the twofold axis parallel to the diagonal of the (*a*, *b*) face which is vertical in Fig. 10. This surprising observation, that molecules correspond *via* a twofold axis in one crystal form and *via* a screw axis in another crystal, is explained by the geometrical relationships of the two unit cells highlighted above. Furthermore, it can be observed that particular translations along the unit-cell edges of the tetragonal crystal reproduce the 'tetrameric' arrangement shown in Fig. 10 also in the orthorhombic crystal (albeit with a slight shift): these are translations $m \cdot a + n \cdot b$ (tetragonal *a* and *b*) for which $m + n = 2p$. Of course this arrangement does not extend to the volume, and in between these limited specific zones of near coincidence between the two crystal forms, the crystal packing is quite different.

4. Concluding remarks

4.1. *The role of Zn in the class B β-lactamases*

The structure of *B. cereus* β-lactamase at pH 5.6 (Carfi *et al.*, 1995) revealed only one Zn ion (equivalent to Zn1) although the Zn2 ligands are present. Actually the K_d for the second site is 25 m*M* at pH 5.6 (Davies & Abraham, 1974; Baldwin *et al.*, 1978) but is in the micromolar range at pH 7.5 (Paul-Soto, unpublished results). This is in agreement with the observation of two Zn ions in the *B. cereus* β-lactamase structure at pH 7.5 (Carfi *et al.*, in preparation). However, the affinity for the second zinc is much higher in the *B. fragilis* enzyme. These differences

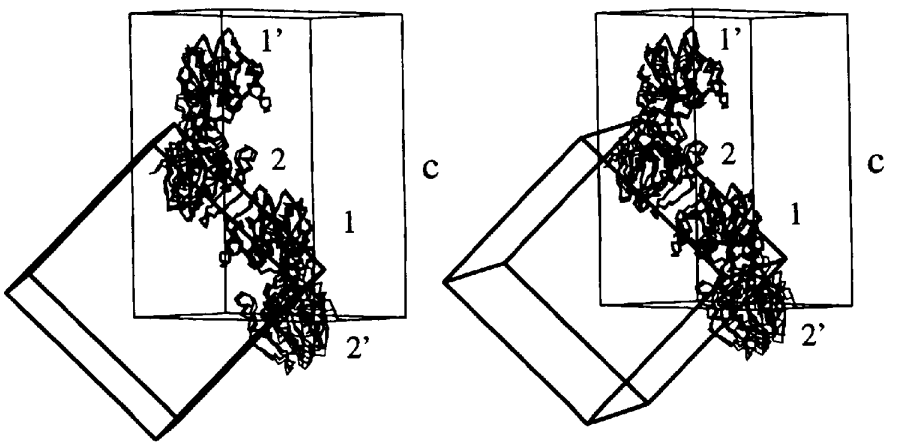

Fig. 10. Correspondence between the tetragonal (thick lines) and orthorhombic (thin lines) crystal forms of the *B. fragilis* metallo-β-lactamase. For clarity, only the *c* axis of the orthorhombic form is labelled, its (*a*, *b*) face being seen edge on. The tetragonal form has its (*a*, *b*) face almost parallel to the figure plane. The asymmetric unit of both crystal forms comprises molecules 1 and 2. Molecules 1′ and 2′ are generated from molecules 1 and 2 by crystallographic symmetry operators which are different in the two crystal forms (see text).

may result from the replacement of Cys87 by an arginine in *B. cereus*. In fact, the guanidinium group of the Arg points towards the second zinc ion (Zn2 ···Arg91 NH2 4.2 Å) and its positive charge may decrease the Zn binding-constant; by contrast the Na^+ ion found in *B. fragilis* β-lactamase is at 6 Å from Zn2 and should not interfere with Zn2 binding. The pH dependent deprotonation of the zinc ligands Cys164 SH and His206 ND1 could account for the increased zinc affinity at basic pH. Finally, it is interesting to observe that the metallo-β-lactamase from *Aeromonas hydrophila*, in spite of the fact that the zinc ligands for the second site are conserved, is active only in its mono zinc form and is reversibly inhibited when the second zinc site is occupied (Hernandez *et al.*, manuscript in preparation). It is worth noting that several zinc proteases are inhibited by excess zinc (*e.g.* thermolysin, carboxypeptidase A, human neutrophil collagenase, angiotensin converting enzyme).

The questions which arise from the structural and biochemical data is the role of the second zinc in the class B enzymes and how the *B. cereus* enzyme can be active both in its mono or dizinc form. A mechanism can be proposed which is compatible with the two situations. We have docked an ampicillin and cephaloridine molecules in the active site of *B. fragilis* β-lactamase (Fig. 11). In our docking the carbonyl O atom of the β-lactam ring interacts with the Asn176 ND2 and the Zn1 (which form the oxyanion hole) and the carboxylate interacts either with the second zinc (2.4 Å) or in its absence with the positively charged His206. A water molecule or hydroxyl ion polarized and positioned by the two zinc and Asp86 OD1, or by the Zn1 and Asp86 OD1 in the mono zinc form, would attack the carbonyl C atom of the β-lactam. Asp86 would conserve its function of proton shuttle, in both cases, as in the mono-zinc enzymes (*e.g.* carboxypeptidase and thermolysin). A similar mechanism was proposed for the binuclear metal enzymes urease ($2Ni^{2+}$) (Jabri, Carr, Hausinger & Karplus, 1995) and arginase ($2Mn^{2+}$) (Kanyo, Scolnick, Ash & Christianson, 1996). In the mechanism proposed by Concha *et al.* (1996) the β-lactam carbonyl O atom also interacts with Asn176 ND2 and the Zn1 but the carboxylate is proposed to make a salt bridge with Lys167 NZ. The role proposed for Lys167 seems unlikely since this residue is not strictly conserved in all sequences. Moreover, according to our docking of two β-lactam antibiotics (Fig. 11) the distance between an O atom of the carboxylate and the charged NZ atom of the lysine ranges between 5.3 and 6.2 Å. The inhibitory effect of the second zinc in the *Aeromonas* enzyme could be due to a change in the conformation of Asp86 (in the *B. fragilis* numbering) upon zinc binding. In the *Aeromonas* enzyme Asp52 is replaced by Gly and this could have an indirect effect (through Arg87) on the optimum position of Asp86 for catalysis when the second zinc ion is present.

The metallo-β-lactamase from *A. hydrophila*, *B. cereus* and *B. fragilis* provide three different pictures. The *A. hydrophila* enzyme is active with one Zn^{II} ion and is

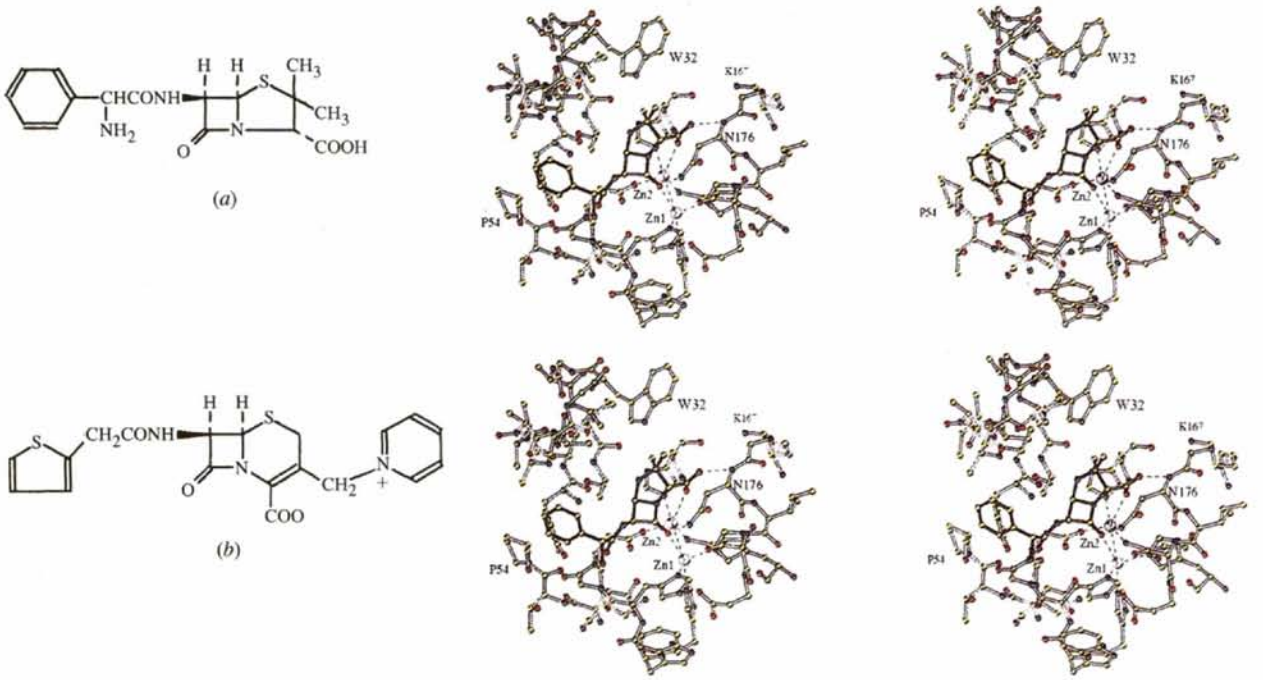

Fig. 11. Stereoview of the docking of β-lactam substrates in the *B. fragilis* β-lactamase active site. The substrates displayed in black are (*a*) ampicillin and (*b*) cephaloridine. The corresponding chemical structures are shown on the left side. Interactions used in the docking procedure (see text) are indicated with a dashed line.

inhibited by the binding of a second zinc ion. The *B. cereus* enzyme is active with one zinc ion and the binding of the second zinc, whose affinity is highly pH dependent, increases its activity. The *B. fragilis* enzyme tightly binds two zinc ions per mol but, as yet, the potential activity of a mono-zinc form remains undetermined. From these observations it seems difficult to conclude, as stated by Concha *et al.* (1996), that metallo-β-lactamases, as a group, are binuclear enzymes. More likely they may present an evolutionary pathway from a mono zinc enzyme (*A. hydrophila*) to an enzyme with one or two zinc ions (*B. cereus*). Therefore, it seems that the presence of a tightly bound second zinc in the *B. fragilis* enzyme is the result of an evolutionary phenomenon and that this second ion is not essential for catalysis in the class B enzymes.

4.2. *Comparison with the structure of B. fragilis β-lactamase in the tetragonal crystal form (Concha et al., 1996)*

Since this paper was submitted, the PDB file for the tetragonal form (1ZNB) was released, allowing for a direct comparison with the orthorhombic form. It confirms the analysis of the tetragonal crystal packing described above. In the tetragonal form, the two molecules *A* and *B* of the asymmetric unit are more similar than in the orthorhombic form, *A* being slightly less open than *B*. The general structure is the same, except for the orientation of some surface side chains. 121 water molecules bound to molecule *A*, and 122 bound to molecule *B* are found in equivalent positions in both crystal forms. However, Asp196 of molecule *B* is differently oriented, without any apparent reason, and does not interact anymore with the Zn1 ligand His101, an interaction important to stabilize the Zn ligands. Furthermore three amino-acid changes, as compared with the known sequence of *B. fragilis* β-lactamase (Thr79 instead of Met, Ala85 for Thr, Lys113 for Arg), are mentioned in the PDB file but were not discussed in Concha *et al.* (1996) where Fig. 4 uses the standard sequence (BLAB_BACFR).

This is publication No. 443 of the Institut de Biologie Structurale Jean-Pierre Ebel (CEA-CNRS). This work was supported by an ECC grant Human Capital and Mobility No. ERBCHRXCT930268, a French IMABIO program and the Belgian Government as part of a Pôle d'Attraction Inter-universitaire (PAI No. 19).

References

Baldwin, G. S., Galdes, A., Hill, H. A. O., Smith, B. E., Waley, S. G. & Abraham, E. P. (1978). *Biochem. J.* **175**, 441–447.

Bernstein, F. C., Koetzle, T. F., Williams, G. J. B., Meyer, E. F. Jr, Brice, M. D., Rodgers, J. R., Kennard, O., Shimanouchi, T. & Tasumi, M. (1977). *J. Mol. Biol.* **112**, 535–542.

Brannigan, J. A., Dodson, G., Duggleby, H. J., Moody, P. C. E., Smith, J. L., Tomchick, D. R. & Murzin, A. G. (1995). *Nature (London)*, **378**, 416–419.

Brünger, A. T. (1992). *X-PLOR Version 3.1: A System for X-ray Crystallography and NMR*, Yale University Press, New Haven, CT, USA.

Carfi, A., Pares, S., Duée, E., Galleni, M., Duez, C., Frère, J.-M. & Dideberg, O. (1995). *EMBO J.* **14**, 4914–4921.

Carfi, A., Paul-Soto, R., Martin, L., Pétillot, Y., Frère, J.-M. & Dideberg, O. (1997). *Acta Cryst.* D**53**, 485–487.

Collaborative Computational Project, Number 4 (1994). *Acta Cryst.* D**50**, 760–763.

Concha, N. O., Rasmussen, B. A., Bush, K. & Herzberg, O. (1996). *Structure*, **4**, 823–836.

Crowder, M. W., Wang, Z., Franklin, S. L., Zovinka, E. P. & Benkovic, S. J. (1996). *Biochemistry*, **35**, 12126–12132.

Das, A. K., Helps, N. R., Cohen, P. T. W. & Barford, D. (1996). *EMBO J.* **15**, 6798–6809.

Davies, R. B. & Abraham, E. P. (1974). *Biochem. J.* **143**, 129–135.

Duée, E., Olivier-Deyris, L., Fanchon, E., Corbier, C., Branlant, G. & Dideberg, O. (1996). *J. Mol. Biol.* **257**, 814–838.

Egloff, M. P., Cohen, P. T., Reinemer, P. & Barford, D. (1995). *J. Mol. Biol.* **254**, 942–959.

Felici, A., Amicosante, G., Oratore, A., Strom, R., Ledent, P., Joris, B., Fanuel, L. & Frère, J.-M. (1993). *Biochem. J.* **291**, 151–155.

Goldberg, J., Huang, H. B., Kwon, Y. G., Greengard, P., Nairn, A. C. & Kuriyan, J. (1995). *Nature (London)*, **376**, 745–753.

Griffith, J. P., Kim, E. E., Sintchak, M. D., Thomson, J. A., Fitzgibbon, M. J., Fleming, M. A., Caron, P. R., Hsiao, K. & Navia, M. A. (1995). *Cell*, **82**, 507–522.

Holland, D. R., Tronrud, D. E., Pley, H. W., Flaherty, K. M., Stark, W., Jansonius, J. N., McKay, D. B. & Matthews, B. W. (1992). *Biochemistry*, **31**, 11310–11316.

Hutchinson, E. G. & Thornton, J. M. (1990). *Proteins*, **8**, 203–212.

Jabri, E., Carr, M. B., Hausinger, R. P. & Karplus, P. A. (1995). *Science*, **268**, 998–1004.

Jones, T. A., Zou, J.-Y., Cowan, S. W. & Kjeldgaard, M. (1991). *Acta Cryst.* A**47**, 110–119.

Kabsch, W. (1988). *J. Appl. Cryst.* **21**, 916–924.

Kanyo, Z. F., Scolnick, L. R., Ash, D. E. & Christianson, D. W. (1996). *Nature (London)*, **383**, 554–557.

Kissinger, C. R., Parge, H. E., Knighton, D. R., Lewis, C. T., Pelletier, L. A., Tempczyk, A., Kalish, V. J., Tucker, K. D., Showalter, R. E., Moomaw, E. W., Gastinel, L. N., Habuka, N., Chen, X., Maldonado, F., Barker, J. E., Bacquet, R. & Villafranca, J. E. (1995). *Nature (London)*, **378**, 641–644.

Kraulis, P. J. (1991). *J. Appl. Cryst.* **24**, 946–950.

Lamzin, V. S. & Wilson, K. S. (1993). *Acta Cryst.* D**49**, 129–147.

Laskowski, R. A. (1993). *J. Appl. Cryst.* **26**, 283–291.

Mol, C. D., Kuo, C.-F., Thayer, M. M., Cunningham, R. P. & Tainer, J. A. (1995). *Nature (London)*, **374**, 381–386.

Navaza, J. (1994). *Acta Cryst.* A**50**, 157–163.

Oefner, C. & Suck, D. (1986). *J. Mol. Biol.* **192**, 605–632.

Ramachandran, G. N., Ramakrishnan, C. & Sasisekharan, V. (1963). *J. Mol. Biol.* **7**, 95–99.

Read, R. J. (1986). *Acta Cryst.* A**42**, 140–149.

Suck, D., Oefner, C. & Kabsch, W. (1984). *EMBO J.* **3**, 2423–2430.